

# Validation of Photon Sample by Estimating $W^\pm \rightarrow e^\pm\nu$ and $Z \rightarrow e^+e^-$ Cross Sections

Samantha Hewamanage, Jay Dittmann, Nils Krumnack  
*Baylor University*

Raymond Culbertson, Sasha Pronko  
*Fermilab*

## Abstract

We estimate the  $W$  and  $Z$  cross sections using photon-like electron selection cuts to validate the photon data sample used in the  $\gamma + \geq 1$  jet +  $\cancel{E}_T$  model-independent resonance search. The results are in good agreement with the values obtained using the standard electron selection cuts. Both measurements fall within 11% of the expected values.

## 1 Introduction

The photon triggers accept leptons in addition to photons. Most of these leptons are from  $W$  and  $Z$  boson decays. As a cross check of the quality of the data used in the model-independent resonance search in the  $\gamma + \geq 1$  jet +  $\cancel{E}_T$  channel, photon-like electron selection cuts [1] are used to identify the electrons and to estimate the  $W$  and  $Z$  production cross sections in the channels  $W \rightarrow e\nu$  and  $Z \rightarrow e^+e^-$ . No accounting of any background is done in either case.

## 2 Datasets

### 2.1 Data

We use the high- $p_T$  photon datasets `cph10d`, `cph10h`, `cph10i`, and `cph10j` which were collected at CDF during the run periods 0–11 (run range 138425 to 237795) with triggers `PHOTON_ISO_25`, `PHOTON_50`, and `PHOTON_70`. These triggers are high- $p_T$  photon triggers which suit our resonance search. Good run list `goodrun_v17_pho_02` from the Photon Group is used to estimate the luminosity. After the good run selection the total luminosity is  $2034 \text{ pb}^{-1}$ .

### 2.2 Monte Carlo Datasets

Here we use PYTHIA Monte Carlo samples generated by the CDF Electroweak Group. The efficiency and acceptance are calculated from the inclusive  $W \rightarrow e\nu$  data set `wewkge` and  $Z/\gamma^* \rightarrow e^+e^-$  data set `zewkad`.

### 3 Electron Selection Variables

We use photon-like electron ID cuts (Table 1) to identify electrons. As we are trying to validate a photon sample that will be used for a photon analysis, we use photon-like electron ID cuts that are very close to photon ID cuts except that they allow for one extra high- $p_T$  track. Table 1 summarizes these cuts.

#### 3.1 Detector

The CDF detector is divided into three regions: central, plug, and forward. The central part extends from pseudorapidity  $\eta = -1.1$  to  $1.1$  and the plug region extends from  $1.1$  to  $3.5$  and  $-1.1$  to  $-3.5$ . The forward region extends from  $3.5$  to  $5.9$  and  $-3.5$  to  $-5.9$ . The central part of the detector is better instrumented and well understood compared to the other two regions.

#### 3.2 Photon Conversion

We are interested in electrons originating from the primary hard scattering. But there are many other secondary processes that can produce electrons. One such process is pair production by photons. An energetic photon can convert to an electron and a positron pair. Using the tracking information from the Central Outer Tracker (COT), such electrons can be identified and removed with a high efficiency.

The effect of this cut is less in this calculation, as photon ID cuts suppress conversions (electrons in general) significantly by cutting on the number of tracks and the track  $p_T$  (see Section 3.8).

#### 3.3 $E_T$

The  $E_T$  is the transverse component of total energy deposited by the electron in the EM calorimeter. We require electrons to have  $E_T > 30$  GeV.

#### 3.4 Ces Fiducial

These CES requirements are defined by the active region of the detector.  $X_{CES}$  and  $Z_{CES}$  cuts ensure that the energy cluster is well contained. The fiducial region is defined by the CES local coordinates  $|x| < 21$  cm and  $9$  cm  $< |z| < 230$  cm.

#### 3.5 Average $\chi^2$

The  $\chi^2$  value is a measure of the shape of the shower profiles created by different particles. This is obtained by comparing the observed lateral shower shape in the CES strips and wires with the predicted test beam shape. The average of the strips and wires should be  $< 20$ .

#### 3.6 Had/Em

Had/Em is the direct ratio of the total energy in the hadronic calorimeter and the electromagnetic calorimeter of electron energy cluster. Electromagnetic (EM) objects like electrons, positrons, and photons deposit more energy in the EM calorimeter while hadrons deposit more energy in the HAD calorimeter.

### 3.7 $E_T^{Iso(corr)}$ in Cone 0.4

$E_T^{Iso(corr)}$  is defined as

$$E_T^{Iso(corr)} = E_T^{0.4} - E_T^{cluster} \quad (1)$$

where  $E_T^{0.4}$  is the energy in the cone of radius  $\Delta R = \sqrt{\Delta\eta^2 + \Delta\phi^2} \leq 0.4$  around the electron cluster excluding the electron cluster, and  $E_T^{cluster}$  is the energy in the electron cluster. This is a measure of the energy surrounding the object. A well isolated electron occupies 1 or 2 calorimeter towers and there is not much energy outside of the electron cluster, meaning there are no other objects which can compromise identification.

### 3.8 N3D Tracks and Track $p_T$

A track pointing to the energy cluster is the strongest discriminator we have to separate electrons from photons. If there is a clearly identified track, it is most likely an electron. N3D is the number of tracks which hit the calorimeter within 5 cm of the photon seed tower. We allow only one track and its  $p_T$  must be smaller than the  $p_T$  shown in the Table 1.

### 3.9 $E/p$

$E/p$  is the ratio of the energy to momentum of the electron.

### 3.10 Track isolation in cone 0.4

Within the clustering cone of 0.4, there cannot be many tracks pointing to the electron cluster. If there are many tracks, it may not be an electron, but a jet. This puts a constraint on the sum of the transverse momenta of all the tracks within 5 cm of the vertex and  $\Delta R \leq 0.4$  compared to the electron direction.

### 3.11 CES strip and wire cluster

The CES wire cluster selection requires the highest  $E_T$  wire cluster in a “half wedge”, where a half wedge is defined as a half of the wedge on one side of the central detector. The highest  $E_T$  strip cluster must be within 25 cm in  $z$  of the EM centroid.

### 3.12 $|\Delta z|$

The highest  $p_T$  track pointing to the cluster must originate from the primary vertex. In case of multiple vertices, the primary vertex is considered to be the highest sum  $p_T$  vertex. If not, the track could be a fake track or the electron could be from a secondary process. This is a cut on the closest distance from the primary vertex to the extrapolated track and it should be smaller than 3 cm.

## 4 Event Selection

First we list the selection requirements that are common to both  $W$  and  $Z$  events. Then we list additional cuts used in each case separately.

1. The run number must be in the good run list.
2. The event should pass PHOTON\_25\_ISO, PHOTON\_50 or PHOTON\_70 trigger.
3. There should be at least one good class 12 vertex.
4. The  $z$ -coordinate of the highest- $p_T$  vertex should be within the well instrumented region, i.e.  $|z| < 60$  cm.

### 4.1 Additional Selections for $W$

An event satisfying the following additional selection requirements is considered as a  $W$  candidate.

1. We require one reconstructed photon  $E_T > 30$  GeV that passes photon-like electron ID cuts (Table 1). Events with more than one electron candidate are excluded.
2.  $\cancel{E}_T > 20$  GeV (See Fig. 11.) (No correction is made to the missing transverse energy.)

### 4.2 Additional Selections for $Z$

An event is considered a  $Z$  candidate if two reconstructed photons  $E_T > 30$  GeV passing photon-like electron ID cuts (Table 1) are found. Events with more than two such photons are excluded. We do not apply any cut on the  $Z$  mass.

## 5 Efficiency and Acceptance

The product of the efficiency and acceptance is calculated using Monte Carlo data samples and the following formula. This is the ratio between the number of events we identified as  $W$  or  $Z$  and total number of events processed.

$$\text{Efficiency} * \text{Acceptance} = \frac{\text{No. of candidates observed}}{\text{No. of generator level events processed}} \quad (2)$$

We do not correct for trigger efficiency, which we expect to be nearly 100% efficient in the  $E_T > 30$  GeV region. This study will be sensitive to this expectation. In Monte Carlo events, the trigger requirement is dropped as the information is not available.

### 5.1 For $W$

We do not apply any cuts at the generator level. We use the same exact event selection as described in Section 4.1.

$$(\text{Efficiency} * \text{Acceptance})_W = 11.38\% \quad (3)$$

## 5.2 For $Z$

A  $Z$  mass window cut of  $66 < Z_{mass} < 115$  GeV is applied at the generator level for two reasons.

1. The  $E_T$  cut (Table 1) is so high that it virtually removes the Drell-Yan contribution in the data. So this will help to suppress the Drell-Yan in the Monte Carlo sample.
2. To match Reference [2], in order to compare the final result.

The effect of the trigger smearing, which may reduce the number of  $Z$  candidates observed by 3–5%, is ignored.

$$(\text{Efficiency} \times \text{Acceptance})_Z = 3.4\% \quad (4)$$

## 6 Cross Section Measurements (Figures 1, 2 and Table 3)

Cross sections are calculated using the following equation:

$$\text{Cross Section}(\sigma) = \frac{\text{No. of candidates}}{\text{efficiency} \times \text{acceptance} \times \text{luminosity}} \quad (5)$$

The errors are calculated using a simple error estimate:

$$\text{Cross Section Error}(\delta\sigma) = \frac{\sqrt{\text{No. of candidates}}}{\text{efficiency} \times \text{acceptance} \times \text{luminosity}} \quad (6)$$

As for the  $Z$  to  $W$  cross section ratio, the error estimate is as follows:

$$\text{Cross Section Ratio} = \frac{\sigma_Z}{\sigma_W} \quad (7)$$

$$\delta (\text{Cross Section Ratio}) = \frac{\sigma_Z}{\sigma_W} \sqrt{\left(\frac{\delta\sigma_Z}{\sigma_Z}\right)^2 + \left(\frac{\delta\sigma_W}{\sigma_W}\right)^2} \quad (8)$$

Figure 1 shows the calculated  $W$  cross section for each run period. Figure 2 shows the same calculation for  $Z$  bosons. The data in both plots are fitted with linear functions. In general both fits are very poor as there are some significant fluctuations. Figure 3 shows the ratio of the two cross sections for each run period. We observe a better fit and less fluctuation than the individual cross section plots. In Table 3 we have summarized both cross section calculations.

## 7 Conclusion

The  $W$  and  $Z$  cross sections from the linear fits are 3052 pb and 279.3 pb respectively. Both results fall within 11% of the reference values of 2780 pb and 255.8 pb for  $W$  and  $Z$  respectively [2]. We do not see significant run dependency of EM objects in this data sample. This also confirms that we have a good understanding of the electron background in the photon data sample. We assume the variations in the individual cross section plots over run periods are related to the increase in luminosity. The cross section ratio (Figure 3) is very consistent indicating there is no bias in the data. Further we conclude the performance of the photon-like electron selection ID cuts is run independent and the  $E_T$  reconstruction is sufficiently consistent and accurate.

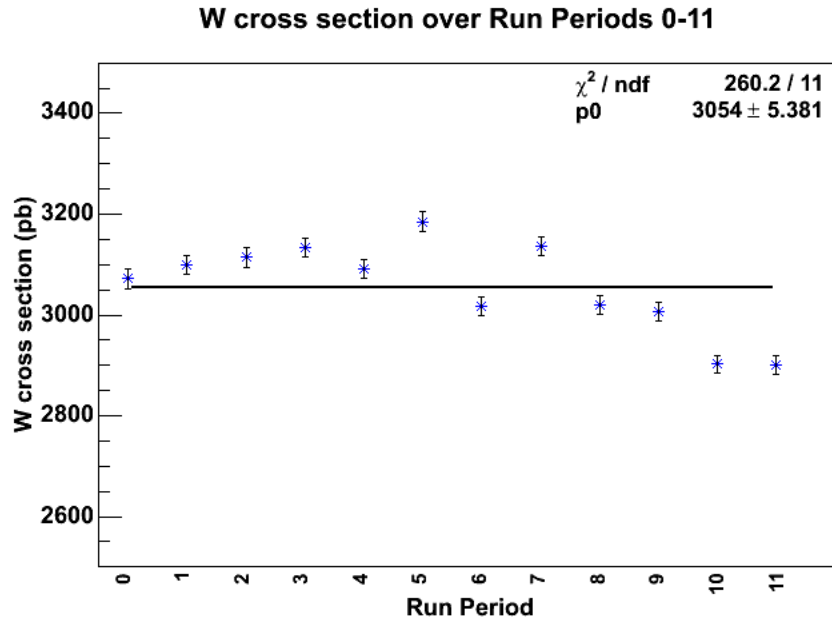


Figure 1:  $W$  cross section over the run periods.

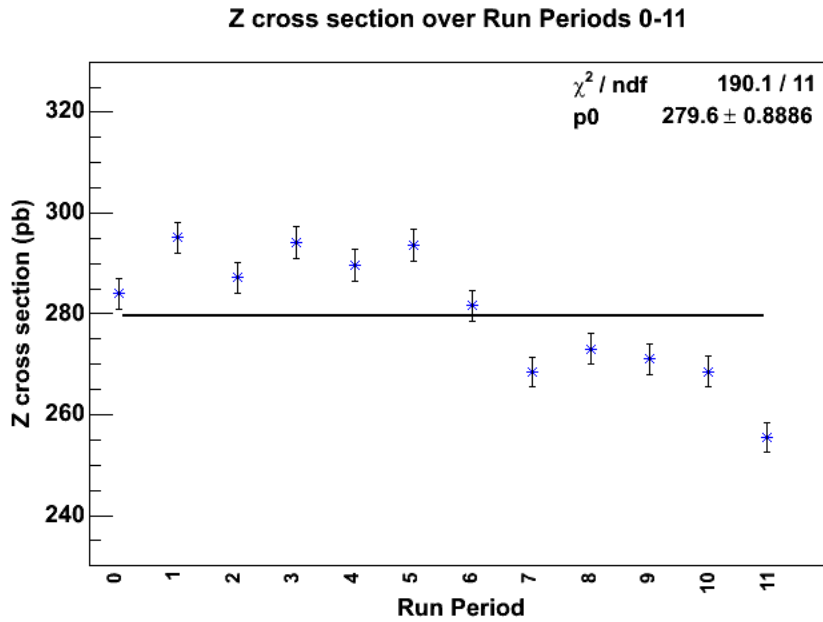


Figure 2:  $Z$  cross section over the run periods.

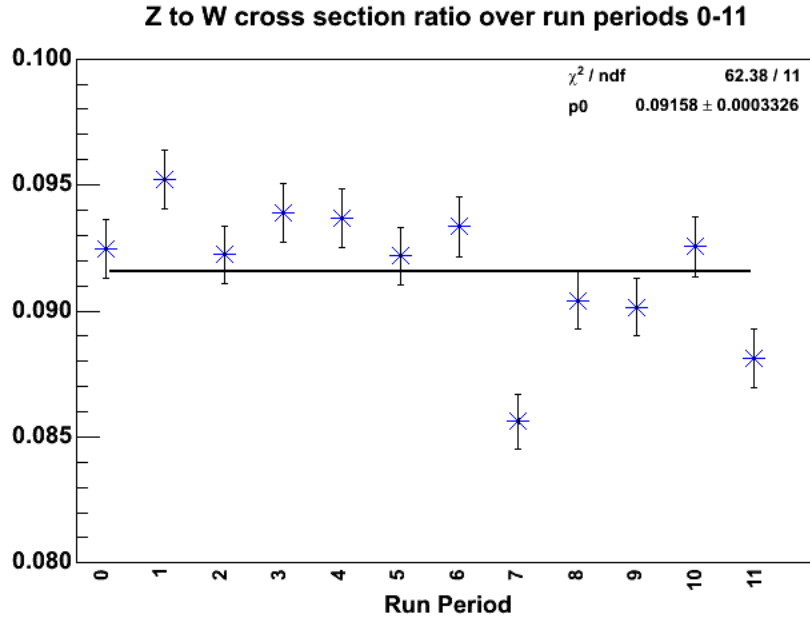


Figure 3:  $Z$  to  $W$  cross section ratio over the run periods.

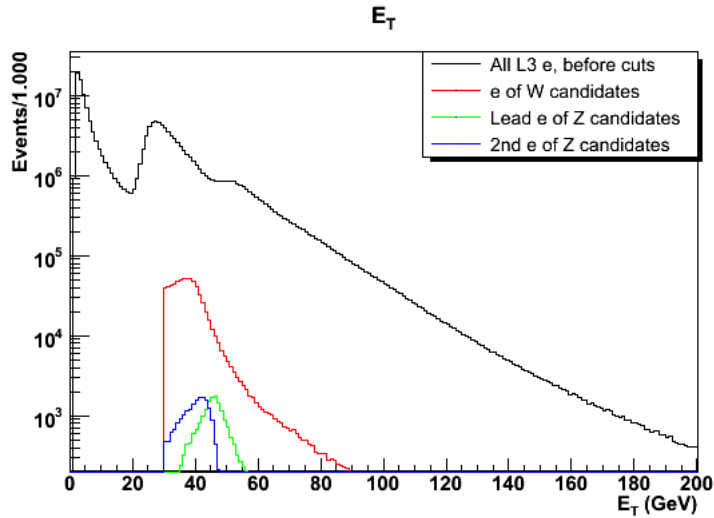


Figure 4: Electron  $E_T$  spectrum.

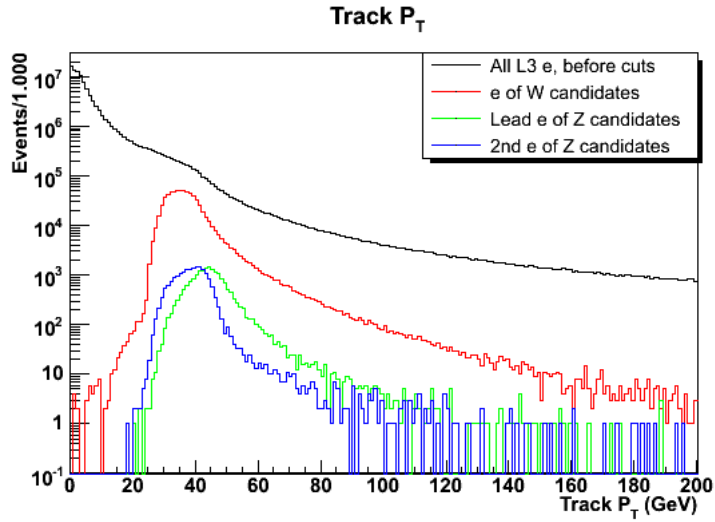


Figure 5: Electron track  $p_T$  spectrum

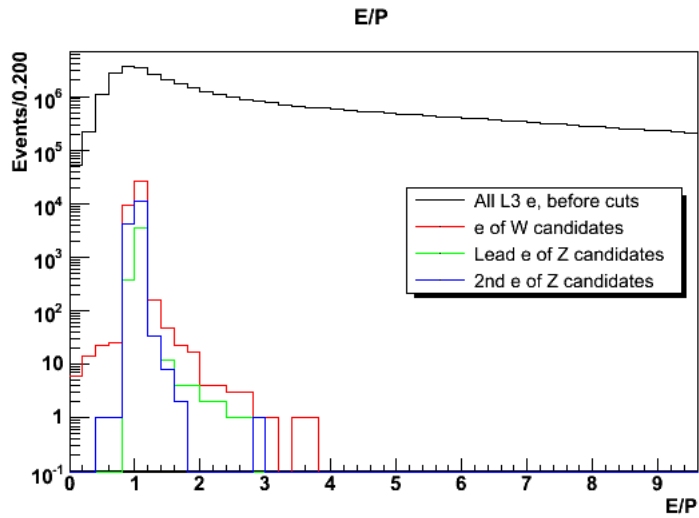


Figure 6: Electron  $E/p$  spectrum

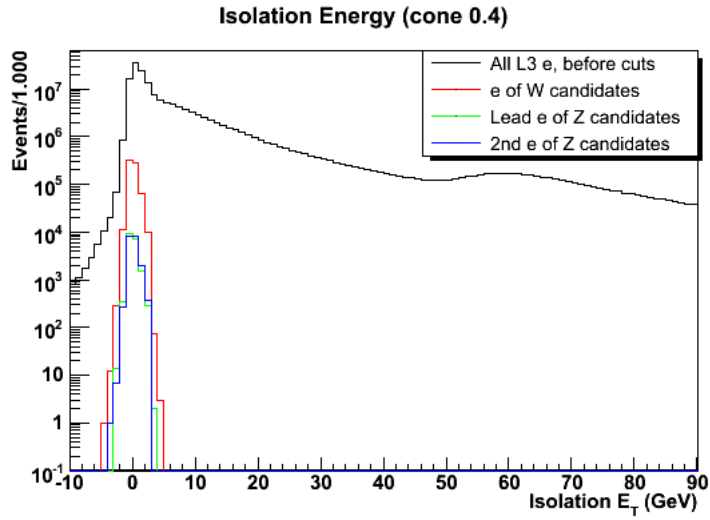


Figure 7: Electron isolation energy (cone size 0.4)

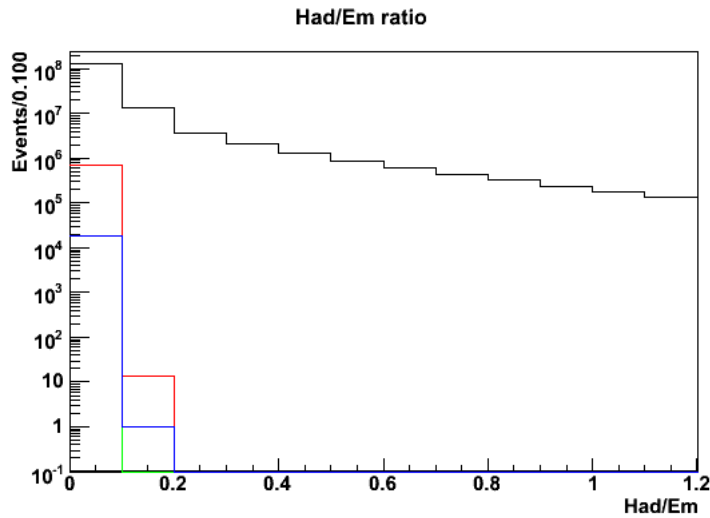


Figure 8: Electron Had/Em energy spectrum

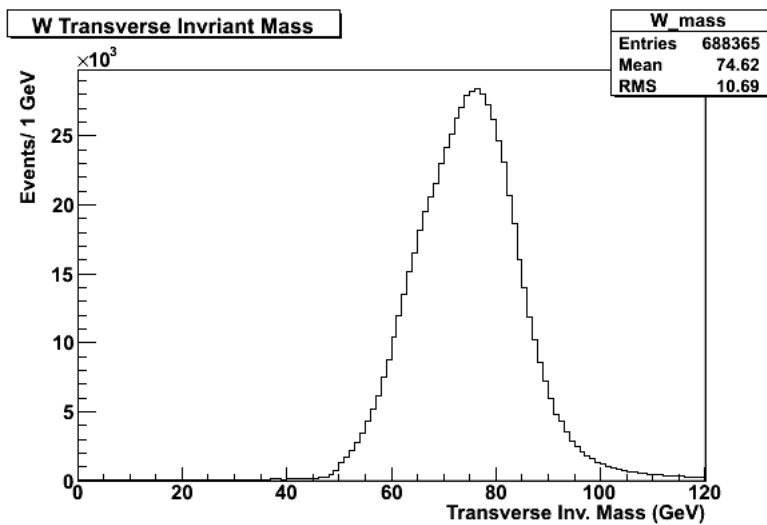


Figure 9:  $W$  transverse invariant mass

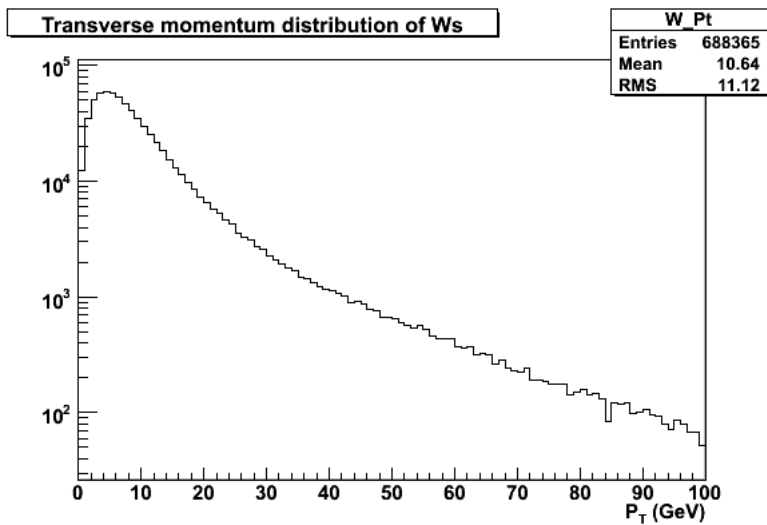


Figure 10:  $W$   $p_T$

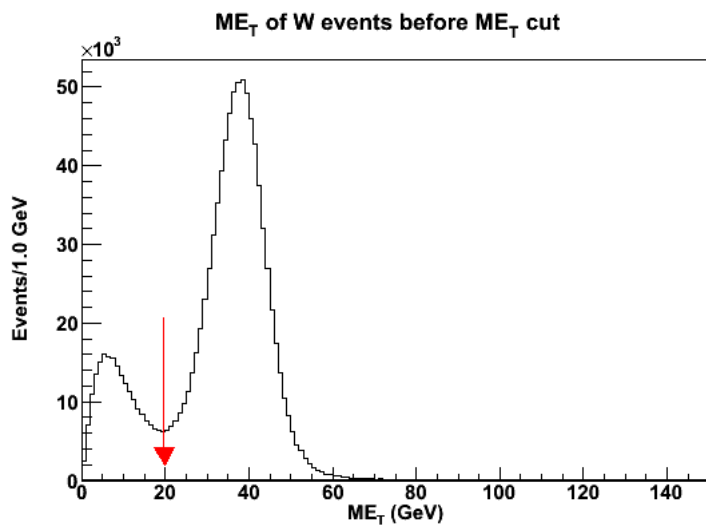


Figure 11:  $\cancel{E}_T$  distribution of  $W$  candidates before cut.

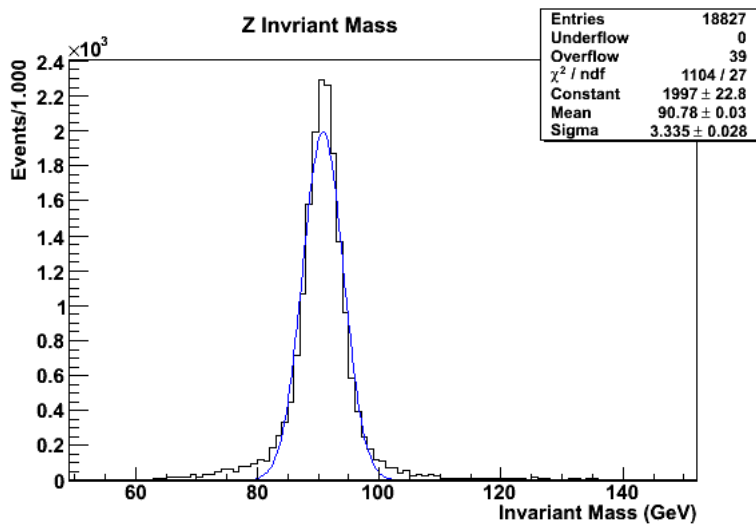


Figure 12:  $Z$  Invariant mass.

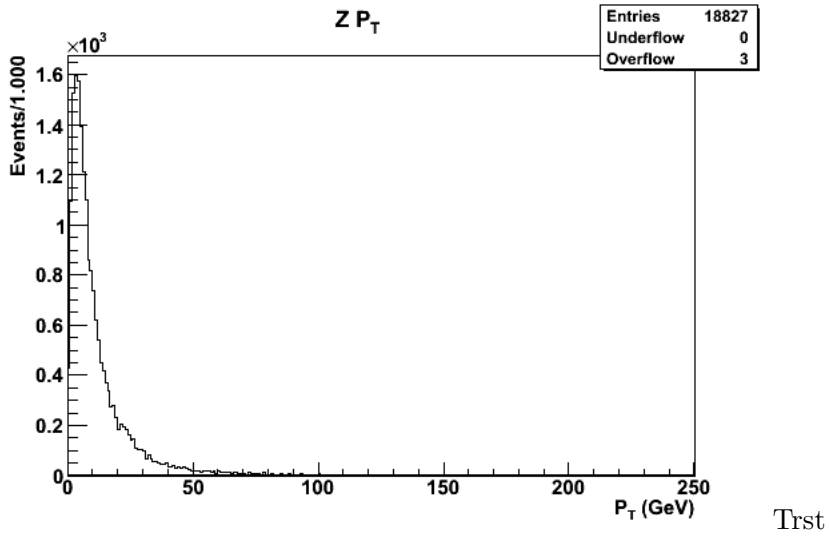


Figure 13: Transverse momentum of  $Z$ .

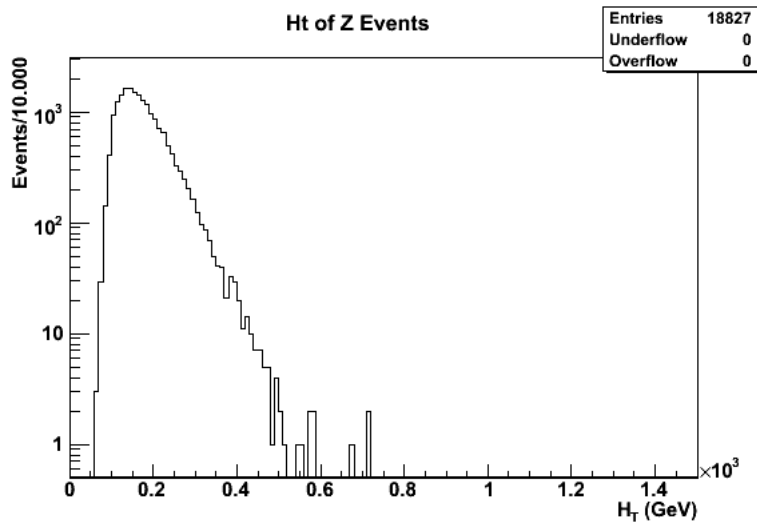


Figure 14:  $H_T$  of  $Z$  Events.

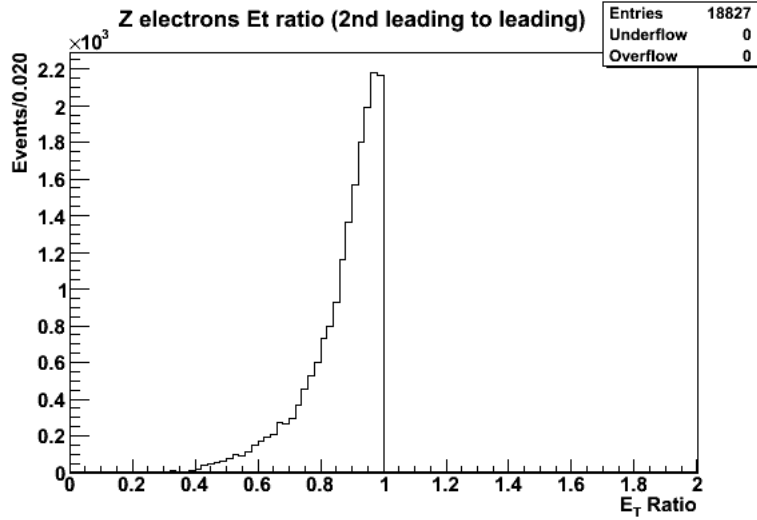


Figure 15:  $E_T$  ratio of two electrons from  $Z$ .

## References

- [1] CDF-8220, R. Culbertson *et al.*, “Probability of an Electron Faking an Isolated Prompt Photon in CEM,” May 30, 2006.
- [2] CDF-6939, D. Acosta *et al.*, (CDF Collab.), “First Measurements of Inclusive  $W$  and  $Z$  Cross Sections from Run II of the Tevatron Collider”, March, 2004
- [3] <http://www-cdf.fnal.gov/tiki/tiki-index.php?page=Stntuple.Datasets.HighPtData>

Variable	Cut value
detector	central
conversion	no
corrected $E_T$	$> 30$ GeV
CES fiduciality	$ X_{CES}  \leq 21$ cm $9 \text{ cm} \leq  Z_{CES}  \leq 230$ cm
average CES $\chi^2$	$\leq 20$
Had/Em	$\leq 0.055 + 0.00045 \times E$
$E_T^{Iso(corr)}$ in cone 0.4	$\leq 0.1 \times E_T$ if $E_T < 20$ GeV $\leq 2.0 + 0.02 \times (E_T - 20)$ if $E_T \geq 20$ GeV
N3D tracks in cluster	$= 1, 2$
$E/p$ of 1st track	$0.8 \leq E/p \leq 1.2$ if $p_T < 50$ GeV no cut if $p_T \geq 50$ GeV
2nd track $p_T$ if N3D = 2	$\leq 1.0 + 0.005 \times E_T$
TrkIso(0.4) - $p_T$ (1st track)	$\leq 2.0 + 0.005 \times E_T$
$E_T$ of 2nd CES cluster (wire and strip)	$\leq 0.14 \times E_T$ if $E_T < 18$ GeV $\leq 2.4 + 0.01 \times E_T$ if $E_T \geq 18$ GeV
$ \Delta z  = z_{vtx} - z_{trk}$	$\leq 3$ cm

Table 1: Photon-like electron ID cuts.

Variable	Candidates
central	94903545
not conversion	87244232
corrected $E_T > 30$ GeV	19369568
Had/Em	16518413
average CES $\chi^2$	12546904
N3D tracks in cluster	5754406
$ \Delta z $	3533572
2nd track $p_T$ if N3D = 2	3035061
$E/p$ of 1st track	1019418
$E_T^{Iso(corr)}$ in cone 0.4	981218
TrkIso(0.4) - $p_T$ (1st track)	981218
$E_T$ of 2nd CES	970328
CES fiduciality	899345
Events with 1 electron	861691
$\cancel{E}_T > 20$ GeV ( $W$ candidates)	689450
Events with 2 electrons ( $Z$ candidates)	18827

Table 2: Event Selection Summary.

Run Period	$W$ candidates	$Z$ candidates	Luminosity ( $pb^{-1}$ )	Cross Section ( $pb$ )	
				$W$	$Z$
0	149283	4111	427	3071.6	284.0
1	42953	1218	121	3099.2	295.1
2	46963	1290	132	3114.1	287.2
3	35941	1005	100	3133.0	294.2
4	30649	855	87	3092.4	289.7
5	47322	1299	130	3185.2	293.6
6	36190	1006	105	3017.3	281.6
7	10158	259	28	3135.6	268.4
8	64839	1746	188	3019.5	273.0
9	57701	1549	168	3006.4	271.0
10	86177	2375	260	2902.1	268.5
11	80593	2115	244	2900.3	255.6

Table 3:  $W$  and  $Z$  cross section calculation summary.